LAWRENCE
LIVERMORE
NATIONAL
LABORATORY

LLNL-JRNL-402553

Dynamic simulations of geologic materials using combined FEM/DEM/SPH analysis

J. P. Morris, S. M. Johnson

March 27, 2008

Geomechanics and Geoengineering

Disclaimer

"Catchline" (i.e. wording at head of first page only) *Geomechanics and Geoengineering*
Vol. X, No. X, Month 200X, 000–000

Running heads (verso) *XXXXXXXXXXXXXXXXXXXXXXXXXXXXXX*

(recto) *Geomechanics and Geoengineering*

ARTICLE TYPE ('SECTION HEAD'**)**

Article Title: Dynamic simulations of geologic materials using combined FEM/DEM/SPH analysis

Joseph Morris[a*] and Scott Johnson[a]

[a]*Atmospheric, Earth, and Energy Division, Lawrence Livermore National Laboratory, Pleasanton, U.S.A.;*

(PLEASE SUPPLY **TWO** TITLE PAGES FOR FIRST SUBMISSION: ONE WITHOUT THE ABOVE AUTHORS, CORRESPONDING
AUTHOR, AFFILIATION AND EMAIL INFORMATION -- FOR BLIND REVIEW -- AND A SECOND CONTAINING THIS INFORMATION
FORMATTED AS ABOVE)

Abstract

An overview of the Lawrence Discrete Element Code (LDEC) is presented, and results from a study investigating the effect of explosive and impact loading on geologic materials using the Livermore Distinct Element Code (LDEC) are detailed. LDEC was initially developed to simulate tunnels and other structures in jointed rock masses using large numbers of polyhedral blocks. Many geophysical applications, such as projectile penetration into rock, concrete targets, and boulder fields, require a combination of continuum and discrete methods in order to predict the formation and interaction of the fragments produced. In an effort to model this class of problems, LDEC now includes implementations of Cosserat point theory and cohesive elements. This approach directly simulates the transition from continuum to discontinuum behavior, thereby allowing for dynamic fracture within a combined finite element/discrete element framework. In addition, there are many application involving geologic materials where fluid-structure interaction is important. To facilitate solution of this class of problems a Smooth Particle Hydrodynamics (SPH) capability has been incorporated into LDEC to simulate fully coupled systems involving geologic materials and a saturating fluid. We will present results from a study of a broad range of geomechanical problems that exercise the various components of LDEC in isolation and in tandem.

Keywords*:* Geomechanics, Fluid-solid coupling, Numerical methods

Title Page Footnote:

*Corresponding author. Email: morris50@llnl.gov

Introduction

A wide range of geological applications involve materials or systems that are discontinuous at fine enough scale of observation. While some systems may be intrinsically discontinuous, other discontinuous systems are best approximated by a continuum, a discontinuum, or a combination of the two, depending upon the specific information of interest. Continuum, mesh-based methods have been applied successfully to many problems in geophysics, and a continuum approximation may be adequate when sufficiently large length scales are considered—even if the geology includes fractures and faults. However, a large class of problems exists where individual rock discontinuities must be taken into account. This includes problems whose structures of interest have sizes comparable with the block size, or when the structures experience loads that do no measurable damage to individual blocks, but deformation along material discontinuities still leads to structural failure. In these cases, a purely continuum, mesh-based treatment is usually inappropriate. Field tests indicate that structural response can be dominated by the effect of preexisting fractures and faults in the rock mass. Consequently, accurate models of underground structures must take into account deformation across fractures and not simply within the intact portions of the rock mass.

The distinct element method (DEM) is naturally suited to simulating such systems because it can explicitly accommodate the blocky nature of natural rock masses. Cundall and Hart (1992) review a number of numerical techniques that have been developed to simulate the behavior of discontinuous systems using DEMs. The distinct element method (DEM) is naturally suited to simulating such systems because it can explicitly accommodate the blocky nature of natural rock masses. Cundall and Hart [1] review a number of numerical techniques that have been developed to simulate the behavior of discontinuous systems using DEMs. In general, an explicit scheme is used to evolve the equations of motion of discrete bodies directly and the bodies may be rigid or deformable. Early approaches employed rigid disks or spheres with compliant contacts [2,3]. Cundall [4], Walton [5] and Cundall and Hart [6] developed two-dimensional DEMs that employed arbitrary polygons. Cundall [7] and Hart et al. [8] also developed fully three-dimensional DEMs composed of rigid or deformable polyhedral blocks with compliant contacts. The DEM has been applied to a wide range of problems in geomechanics (see Cundall [9] for a review of DEM simulations of granular material and rock). The Livermore Distinct Element Code (LDEC) was originally developed to implement DEM capabilities similar to Cundall[7] and Hart et al.[8] (see Morris et al., 2002). LDEC was subsequently used to simulate the response of underground tunnels to dynamic loading (Heuze and Morris, 20??).

Beyond the capabilities of the original DEM, many applications in geophysics require a combined continuum-discontinuum treatment for a complete solution. For example, projectile penetration into a rock or concrete target requires continuum-discontinuum analysis in order to predict the formation and interaction of the fragments produced. Underground structures in jointed rock subjected to explosive loading can fail due to both rock motion along preexisting interfaces and fracture of the intact rock mass itself. In such applications, it is insufficient to simply predict whether or not the rock mass will fail—instead, the critical issues are how fracture and discontinuous interaction lead to the ultimate fate of rock fragments. Munjiza (2004) reviews the issues involved in developing combined DEM-FEM capabilities. To answer these questions, a continuum-discontinuum capability was developed by incorporating finite element analysis into LDEC (Morris et al., 2006). LDEC has also been extended to include a nodal cohesive element formulation that allows the study of fracture problems in the continuum-discontinuum setting with reduced mesh dependence (Block et al., 2007).

There are many application involving geologic materials where fluid-structure interaction is important. For example, simulating the near source region of an explosion in rock requires incorporating details of the coupling between the expanding products and the surrounding rock. To facilitate solution of these classes of problem, a Smooth Particle Hydrodynamics (SPH) capability was incorporated into LDEC.

The following sections document the treatments for geologic media and fluid within LDEC in more detail. This is followed by a number of verification problems which test combinations of the capabilities within LDEC. We present simulations of fracture and fragmentation for the case of a shock wave impacting an underground tunnel system which highlights the influence of persistent and non-persistent joint sets on failure in rock. Results of studies investigating impacts into boulder fields and waves impinging upon a breakwater are also presented.

Treatment of geologic media using LDEC

In the simplest case, the Livermore Distinct Element Code can be run in a rigid-block mode, so that all deformation in the system is lumped into the contacts. The most complicated aspect of the code is then related to contact detection. In general, the equations of motion of the elements are determined in a standard manner by integrating vector equations for both the center of mass of each element and an orthonormal vector triad that determines its absolute orientation. Contact detection monitors how the connectivity

changes as a result of relative block motion. The Lagrangian nature of the DEM also simplifies tracking of material properties as blocks move, and it is possible to guarantee exact conservation of linear and angular momentum throughout the computation.

Deformation within the individual blocks is often introduced into DEM formulations by using additional standard continuum discretization, such as finite differences or finite elements. In Morris et al. (2004), it was observed that the theory of a Cosserat point (Rubin, 1995, 2000) can model each element as a homogenously deformable continuum. A Cosserat point describes the dynamic response of the polyhedral rock block by enforcing a balance of linear momentum to determine the motion of the center of mass, as well as three vector balance laws of director momentum to determine a triad of deformable vectors, which model both the orientation of the element and its deformation. The response of the deformable polyhedral block is modelled explicitly using the standard nonlinear constitutive equations that characterize the original three-dimensional material. Consequently, the constitutive equations for the contact forces at the joints become pure measures of the mechanics of joints. However, this approach is inappropriate for problems whose length scales of interest (such as a tunnel diameter) are only slightly greater than the block size. This deficiency was overcome by internally discretizing the polyhedral blocks with a collection of smaller tetrahedral elements. The numerical solution procedure depends on nodal balance laws to determine the motion of the four nodes of each tetrahedral element, similar to that described above for the motion of blocks. In general, the accelerations of the nodes of a particular element are coupled with the nodes of the neighbouring elements. However, the director inertia coefficients in the theory of a Cosserat point can be specified so that these equations become uncoupled. This form corresponds to a lumped mass assumption and is particularly convenient for wave propagation problems using explicit integration schemes because it does not require the inversion of a mass matrix.

In continuum regions, where the nodes of neighbouring elements are forced to remain common (i.e., unbreakable), this meshed based Cosserat point formulation is basically the same as standard finite element models (FEM) that use homogeneously deformable tetrahedral elements. In this case, the computational effort in LDEC is significantly reduced: many nodes are shared and there is no need for contact detection on shared element surfaces. While standard finite element formulations are based on shape functions and weighting functions, the latest version of LDEC utilizes balance laws for the directors of each Cosserat point (associated with the positions of the nodes of the tetrahedral elements). LDEC can be run simultaneously in DEM and FEM-like modes, dynamically blending continuum and discrete regions, as necessary.

It is well known that the simulated fracture propagation rate is highly mesh dependent unless steps are taken to reduce the influence of element size. For simulation of crack growth at the meso- and macro-scale, a cohesive elements is often introduced into a finite element mesh to capture the micromechanical processes leading to material failure. LDEC has been extended to include a nodal cohesive element formulation that allows the study of fracture problems in the continuum-discontinuum setting with reduced mesh dependence (Block et al., 2007).

Although versatile, finite element discretization, with the option of dynamically breaking the mesh introduces significant computational expense. In addition, the current implementation in LDEC restricts crack orientations to follow mesh interfaces which artificially constrains failure propagation, especially for low resolution meshes. Such an approach is unsuitable for applications involving very large numbers of distinct objects undergoing brittle fracture, such as impact into a pile of boulders. For this class of problem, we introduce a constitutive model of fracture utilizing the average stress within each body in the problem using, for example, a von Mises failure criterion. This failure criterion determines whether fracture occurs in this model. Once fracture has been identified, the body is instantaneously split along the plane of greatest tensile principal stress, as determined through the Eigenvectors of the stress tensor. If the uniformly deformable, Cosserat blocks are employed, each block already has an estimate of its internal stress state. If the rigid block formulation is used, a stress estimate may be obtained from the Cosserat formulation by considering the limit of instantaneous equilibrium between the internal state of the block and the applied forces. We use a rigid body stress relation based on the homogeneous deformation of a body in the limit of rigidity.

Smooth Particle Hydrodynamics

Smooth particle hydrodynamics (Monaghan, 1992) is a Lagrangian CFD technique that has found a wide range of applications, including free-surface flows (Monaghan, 1994) and elasticity (Gray et al, 2001). It has also been applied to low Reynolds number flows (Morris et al, 1997), including surface tension (Morris, 2000).

Using SPH a fluid is represented by particles, typically of fixed mass, which follow the fluid motion, advect contact discontinuities, preserve Galilean invariance, and reduce computational diffusion of various quantities including momentum. The equations governing the evolution of the fluid become expressions for interparticle forces and fluxes when written in SPH form. The Lagrangian nature of SPH facilitates coupling to other Lagrangian techniques, such as the DEM.

Using SPH a fluid is represented by particles, typically of fixed mass, which follow the fluid motion, advect contact discontinuities, preserve Galilean invariance, and reduce computational diffusion of various quantities including momentum. The equations governing the evolution of the fluid become expressions for interparticle forces and fluxes when written in SPH form. Using the standard approach to SPH [1] the particles (which may also be regarded as interpolation points) move with the local fluid velocity.

Each particle carries mass, velocity **v**, and other fluid quantities specific to a given problem. The equations governing the evolution of fluid quantities are expressed as summation interpolants using a kernel function with smoothing length.
To simulate fully-coupled interactions between fluids and solids we need to introduce a force between the SPH particles and the DEM polyhedral blocks. LDEC supports two approaches to this coupling: A penalty method and a ghost particle approach.
Using the penalty method, a signed distance, D, is calculated for all SPH particles in the vicinity of a given block above each face of the block. A linear force is applied to the particle that is proportional to the distance the particle penetrates within a chosen stand-off distance, D_0, of the block:

$$\mathbf{F}^{BC} = K^{BC}(D - D_0)\mathbf{n} \qquad \text{EQ 12}$$

The stiffness of the penalty force should be scaled according to the properties of the SPH particle:

$$K^{BC} = A\frac{m\,c^2}{h^2} \qquad \text{EQ 13}$$

Here, A is a non-dimensional constant that controls the amount of penetration of the particles within the stand-off distance D_0 and **n** is the normal to the block. The particle mass, soundspeed and smoothing length are denoted by m, c and h respectively.
The ghost particle approach proceeds by initializing the problem with SPH particles within the solid and fluid regions throughout the computational domain. SPH particles that are initialized inside a solid become "bound" to that solid and are used to provide boundary conditions on the unbound, surrounding SPH particles. This approach has been used successfully to simulate fluid-solid coupling in porous media with SPH (Morris et al, 1997).

Verification simulations

Simulation of a bursting dam

To verify that the LDEC implementation of SPH is consistent with previous studies we reproduced the bursting dam simulation performed by Monaghan [23]. This is a two-dimensional test where initial conditions correspond to a 25m by 25m square cross-sectioned body of water, bounded on its left and from below by free-slip boundaries. The water is allowed to flow in response to the forces of gravity. Figure 2 shows the flow simulated by LDEC's SPH capability using an initial lattice of particles with 0.5m spacing. The free-slip boundaries were modelled using lines of 1m sized rigid LDEC blocks. Figure 3 shows a comparison between our simulations, those of Monaghan [23] and experiments performed by Martin and Noyce [32]. Our results are in good agreement, confirming the implementation of SPH and the free-slip block-SPH particle force in LDEC.

Explosion in limestone

To verify the implementation of SPH and coupling with the FEM capability under dynamic loading in LDEC we simulated a spherical explosion in Limestone and compared results with an established Eulerian adaptive mesh code, GEODYN (Lomov et al., 2001). The computational domain consisted of a 19.8mm radius sphere of CompB explosive embedded in a 100mm radius sphere of Limestone. At t=0, the entire volume of explosive is detonated. The GEODYN code was run in 1-dimensional mode, with a cell size of 1mm. The LDEC code was run in 3-D mode, with the Limestone discretized into tetrahedral elements of side length approximately 10mm. The high explosive in the LDEC simulation was represented by SPH particles initially placed on a cubic lattice of spacing 2mm. The coupling between solid and gas was achieved by using the penalty approach implementation. Figure 1 shows a comparison between the LDEC simulation and GEODYN at several distances from the source. The two methods agree well in terms of peak velocity and waveform. These results verify the LDEC treatment for the expanding gas and treatment of the coupling between the gas and solid.

Dynamic loading of underground structures

Simulations of an underground facility in heavily fractured rock

A series of simulations were performed with LDEC to model the effects of a surface explosion (and the subsequent shock wave) on an underground tunnel system surrounded by jointed rock. The solution domain spanned 60 m in each direction and encapsulated a generic facility that included several tunnel sections and a lift shaft (see Figure 5). Several geological models were considered as part of this study. In particular, the behaviour of regular, persistent joints was compared to the effect of non-persistent (i.e., randomized) joints in the surrounding rock. The rigid block capability was used to model hard rock and as is appropriate for hard rock where joint geometry dominates structural response. Figure 6 shows an example of the randomized jointing present in the non-

persistent model geology. In both cases discussed here, the joint patterns resulted in typical block sizes of 30 cm. Consequently, each model contained approximately 8 million individual polyhedral rock blocks and approximately 100 million contact elements, making these the largest simulations of this type performed to date. The facilities were subjected to loading corresponding to a one kiloton detonation at the surface 50 m above. For this study, waveforms approximating the groundshock were applied as boundary conditions to the computational domain. This approach assumes that the loading of the computational domain can be uncoupled from the response of the facility itself. In contrast, the following section discusses and example where the detonation and tunnel response are more directly coupled.

Figure 7 compares the velocity fields of the two simulations at 30 ms. Results obtained for the regular, persistent joint set and irregular, non-persistent model differed in several key ways:

The regular model exhibited strong anisotropy. Since the joints are weak under shear loading, the regular, persistent joint sets tend to channel the waveform, resulting in variations in wavespeed with direction of propagation.

The irregular model exhibited higher attenuation. Again, because the joints are weak under shear loading, the irregular joint structure results in more effective plastic deformation on the joints and, consequently, more attenuation.

Persistent joints allow shear motion along the entire length of the computational domain, resulting in large "chimney" effects above collapsed tunnels sections.

The irregular model resulted in more diffraction of waves around cavities in the rock mass.

Figure 8 shows two snapshots of the collapse of the largest room within the facility using the non-persistent joint set simulation. While the largest room within the facility has totally collapsed, the narrowest access tunnels experienced minimal damage. The midsize tunnels show a range of damage, with most damage occurring in tunnel sections that contain a junction with another tunnel or lift shaft. This behavior is consistent with the idea that tunnel junctions compromise tunnel strength.

Simulation of a tunnel in infrequently jointed rock

The initial applications of LDEC typically involved a tunnel in heavily jointed, hard rock, where the tunnel diameter was spanned by many blocks (Morris et al. 2002, 2004). It is then appropriate to simulate the rock mass using a "tight" structure consisting of polyhedral blocks that are either rigid or homogenously deformable (with deformable points of contact in either case) such as in the previous section. In contrast, this section considers the response of a tunnel to a detonation, where the joints are sufficiently infrequent so that the predominant failure mechanism is block breakage rather than intact rock displacement. In addition, this problem includes an explosion sufficiently close to the tunnel that it cannot be effectively modelled by a decoupled boundary condition. The detonation is simulated using SPH using the penalty approach for coupling. Consequently, this problem demonstrates the fully-coupled, SPH-FEM-DEM capability of LDEC.

This demonstration simulation (see Figure 2) is performed in two dimensions. The geology consists of blocks of limestone, measuring 1.83 m wide, by 0.30 m high, surrounding a tunnel measuring 1.23 m by 1.23 m, located 1 m below the surface. The tunnel is subjected to loading from a cylinder of CompB high explosive located near the tunnel of radius 0.25m, centered 0.5 m above the ground. The calculation was performed in two stages. Initially, LDEC was run with deformable blocks of limestone internally discretized into 10 cm tetrahedral elements. In this mode of operation, the time step is quite short so that deformation within the 10 cm elements can be captured. After 1 ms, the LDEC calculation was switched over to rigid-block mode, which ignores internal modes of the elements, leading to an increase in the size of the time steps. This allows us to investigate the flow of rubble into the tunnel over longer time scales. Subsequent panels in Figure 2 depict a portion of the roof collapsing into the tunnel.

Impact into a pile of boulders

The design of munitions that can withstand impact into a target with heterogeneities of similar length scale as the projectile has proven to be a persistent and difficult challenge. The stresses induced by these types of impact events are often highly discontinuous, producing bending moments and torsion on the projectile which can exceed design specifications. The situation is complicated by the limited experimental and numerical tools available to improve the design constraints. Experiments are often plagued by challenges, including characterization of the initial conditions, monitoring of the event at sufficient temporal and spatial resolutions, and analysis, which is confounded by the interaction of several chained stochastic impact events before projectile fate is determinate. Simulation tools can overcome these limitations, but they introduce other constraints such as computational tractability (run time and processor availability) and physical model fidelity. Also, the types of simulation approaches that may be effectively applied to this problem are constrained by the discontinuous and anisotropic nature of the medium; the relatively low ratio of resolution length to discontinuity length; and the stochastic nature of the outcome. These constraints, for instance, preclude the use of traditional finite element approaches and make many discontinuous mechanics approaches too costly to run.

Distinct element and combined distinct-finite element methods are designed to address systems where the discontinuities dominate the behavior of the system. DEM approaches [1] have been used in the past to analyze impact events into boulder screens; however,

these analyses were limited to 2-D approximations. The study detailed here analyzes the impact of a projectile into a boulder screen using a 3-D DEM representation of the boulder field with fracture criteria based on plane of maximum tensile stress combined with an empirical model of contact pulverization derived from experimental results [2].

Sensitivity studies indicate the final orientation and position of the projectile are insensitive to the user-defined proportionality constant. Because the resultant fracture is two-dimensional, the contact is poorly defined at the interface of the projectile and boulder. This results in indeterminacy of the resulting trajectory of the produced fragments. To overcome this problem, an empirical model of material comminution (pulverization) at the impact point based on the experimental results of Kumano and Goldsmith [2] has been introduced. The results indicate that for projectiles with flat and spherical tips the equivalent cone angle is marginally higher (i.e., the ratio of depth of penetration to crater volume is lower) than for those with conical tips; however, this small deviation (distribution median of 59° versus 61°) does not impact the final distribution of results. A single assumed angle of 60° is used throughout the simulation for determining the conical comminuted region at impact. Using this angle, the fracture algorithm is amended to fragment the body into quadrants with both split planes oriented along the axis of most tensile principal stress and parallel to the secondary and tertiary principal tensile stress directions, respectively. The split is initiated at the point of the largest magnitude force on the body, and the material at this point is excavated to create the equivalent of a 60° circular cone. The application of a small area load at the point of impact also increases the effective stress at the impact point, requiring an adjustment of the failure stress criterion to account for the increased stress at the impact point. Because the exact geometry of the excavated area is unknown, and the stress concentration factor is sensitive to small changes in geometry, a parametric approach was adopted to determine an effective stress concentration factor. An illustration of the algorithm as applied to a single brittle, granitic block is shown in Figure 3.

As shown in Figure 4, the system is initialized using a randomly-oriented set of rigid cuboids where the dimensions of the cuboids are sampled from a distribution corresponding to those reported in a set of experimental studies [8, 9]. The positions of the elements are initialized on a hexagonal grid with small stochastic deviations from the exact positions. The cuboids are allowed to settle into a trough of trapezoidal cross-section until the residual kinetic energy reaches a threshold at which point the remaining granular temperature is removed. This procedure is reproduced for 10 different realizations of the initial conditions.

The front wall is removed, and the projectile is given an initial velocity and positioned at the impact point. A characteristic simulation progression is shown in Figure 5 for a slice through the fire line and where the normal to the view plane is perpendicular to the gravity vector and the fire line. The blocks are rendered translucently to illustrate the flight path and relative density of the material. The impact event is characterized by a wide distribution in the outcomes for different samples of randomly oriented blocks with the same initial conditions in the projectile. The fate of the projectile at different points in time (pre-impact, directly after impact, and final state) are shown in Figure 6, showing a clear cone of path divergence as a function of path length.

The tortuosity of the projectile path is also an interesting quantity, as projectile erosion and damage is also influenced by the path length traveled through the material. The boulder size relative to the projectile can have a pronounced effect on the ballistic efficiency of the projectile. For the large boulder case, it can be seen in Figure 7 that despite the relatively comparable bulk densities of the large and small boulder systems, the efficiency of the large boulder screen is far in excess of that of the small boulder screen.

These studies illustrate the power of using the LDEC combined DEM/FEM code for predicting distributions of outcomes to projectile impact events in granular materials. Not only can these types of methods provide insight into the basic micromechanics of impact into granular materials, but the fast fracture algorithm detailed here combined with the rigid body stress failure criterion can also rapidly provide error bounds for ballistic efficiency predictions for projectiles, with the predictions calibrated for specific particulate materials.

Despite the low fidelity of the physical approximations used, the distribution of results predicted in this study includes the results found in earlier experimental studies [8, 9].

Coupled fluid-solid simulation: Wave impinging upon a breakwater

Breakwaters are structures intended to dissipate wave energy in order to protect harbours and coastal structures. Latham et al. (elsewhere in this issue) provide a detailed description of several designs for breakwaters using both natural rock and precast concrete armour units. The challenge is to predict the effectiveness of such structures against infrequent, yet potentially catastrophic events such as a 100-year storm. A complete understanding of the performance of these structures must include the possibility of relative motion between the breakwater units and estimation of the internal stress within each unit, including the possibility of unit failure. Latham et al. present an approach for simulating this coupled problem using an Eulerian flow code to simulate the water and Lagrangian DEM to simulate the armour units. The benefit of such an approach is that the methods employed are utilized for the portions of the problem that play to their strengths. An Eulerian CFD code is naturally suited to simulating the large deformations associated with wave motion and a DEM/FEM capability is appropriate for simulating the motion and potential failure of the pile of armour units. The difficulty is that coupling Euler-Lagrange capabilities inevitably requires significant algorithmic complexity. In contrast, coupling Lagrangian capabilities is relatively simple from an algorithmic perspective. The challenge is that the Lagrangian

flow solver employed must be immune to mesh tangling. Despite being more difficult to implement, a fully coupled Euler-Lagrange representation of this problem has distinct advantages. In particular, the Euler component provides a framework for adaptive meshing, permitting a more accurate and potentially more efficient solution of the fluid motion than a fixed resolution SPH calculation would.
We present preliminary calculations of a wave striking a simple breakwater constructed of rigid DEM cubic blocks. The fluid is represented by SPH in order to avoid mesh tangling using the techniques described previously. In contrast with Latham et al., this study did not include the possibility of unit breakage, however, that could be handled using the FEM/DEM capability in LDEC demonstrated in previous sections. Figure ?? shows the results of a simulation of a breakwater using LDEC. The initial boulder pile was created by dropping a number of cubic blocks onto a flat surface bounded with rigid walls on four sides. Subsequently, the water was introduced into the simulation and coupling to the blocks was achieved by using the ghost particle method described previously. After several seconds of settling, a large wave was introduced from the right. The wave impinges upon the breakwater and displaces several blocks from the top of the pile, demonstrating the fully coupled nature of the simulation.

Conclusions

Previous work has demonstrated that the Livermore Distinct Element Code is capable of simulating the dynamic response of elaborate, underground facilities and tunnel systems to shock-wave loading (Morris et al, 2006; Heuze and Morris, 2007). Such large-scale studies allow the investigation of the interaction between different parts of the facility, and the study of how these interactions lead to tunnel collapse and overall failure. The results highlight the importance of including realistic irregular, non-persistent joint sets. Geologies that were modeled using rigid blocks with deformable contacts and non-persistent jointing were found to withstand significantly more shear deformation than would be predicted using regular, fully persistant joint sets. Moreover, discretizing the blocks internally with tetrahedral elements increases the potential accuracy of large-deformation simulations, especially in cases where the predominant failure mechanism is block breakage rather than intact rock displacement. The addition of an SPH capability allows us to simulate detonation close to a tunnel opening, including fracture and fragmentation.
In addition, this paper has demonstrated the internal discretization of the LDEC blocks into tetrahedral elements for cases where the predominant failure mechanism is block breakage rather than intact rock displacement. The addition of an SPH capability allows us to simulate detonation close to a tunnel opening, including fracture and fragmentation.
The current version of LDEC provides simultaneous DEM and FEM-like domain partitioning, as well as the possibility of converting between the two modes dynamically.
EXPAND UPON APPLICATIONS

Acknowledgements

This work was performed under the auspices of the U.S. Department of Energy by Lawrence Livermore National Laboratory in part under Contract W-7405-Eng-48 and in part under Contract DE-AC52-07NA27344.
Also, the authors would like to acknowledge helpful discussions with L. Glenn, M. B. Rubin and T. Antoun.

References

Block, G., Rubin, M.B., Morris, J., Berryman, J.G., Simulations of dynamic crack propagation in brittle materials using nodal cohesive forces and continuum damage mechanics in the dinstinct element code LDEC, *International Journal of* Fracture, 2007, in press.

Cundall, P. A. and Hart, D. H., Numerical modeling of discontinua, *Eng. Comput*., **9**, 1992, 101-113

Gray, J. P., Monaghan, J. J. and Swift, R. P., SPH elastic dynamics, *Comput. Methods Appl. Mech. Engrg.* **190,** 2001, 6641-6662.

Monaghan, J. J., Smoothed Particle Hydrodynamics, *Annual Reviews in Astronomy and Astrophysics*, **30**, 1992, 543-574

Monaghan, J. J., , Simulating Free Surface Flows with SPH, Journal of Computational Physics, 110, 1994, 399-406

Morris, J.P., Fox, P.J., and Zhu, Y., Modeling low Reynolds number flows using SPH, *J. Comput. Phys*. **136**, 1997, 214-226

Morris, J. P., Simulating surface tension with Smoothed Particle Hydrodynamics, *Int. J. Numer. Meth. Fluid Flow*, **33**, 2000, 333-353.

Morris, J. P., Glenn, L. A., and Blair, S. C., The distinct element method - application to structures in jointed rock, in Lecture Notes in Computational Science and Engineering: Meshfree Methods, **26**, Springer-Verlag, Heidelberg, 2002, pp. 291-306.

Morris, J. P., Rubin, M. B., Blair, S. C., Glenn, L. A., and Heuze, F. E., Simulations of underground structures subjected to dynamic loading using the distinct element method, *Engng Comput.*, **21**, 2004, 384-408.

Morris, J. P., Rubin, M. B., Block, G. I., Bonner, M.P., Simulations of Fracture and Fragmentation of Geologic Materials using Combined FEM/DEM Analysis, *International Journal of Impact Engineering*, **33**, 2006, 463-473

Rubin, M. B., Numerical solution of two- and three-dimensional thermomechanical problems using the theory of a Cosserat point, *J. of Math. and Phys*. (*ZAMP*), **46**,

Rubin, M. B. Cosserat Theories: Shells, Rods and Points, Solid Mechanics and its Applications, Kluwer, The Netherlands, 2000.

Munjiza, A., (2004) *The Combined Finite-Discrete Element Method*, John Wiley & Sons.

Lomov, I., Antoun, T., Glenn, L. (2001), "Explosion in the granite field: hardening and softening behavior in rocks", *Proceedings of 12th APS Topical Conference, Shock Compression of Condensed Matter*, Atlanta, Georgia, 24-29 June 2001, .

[**Error! Reference source not found.**] Cundall, P. A. and Hart, D. H. (1992), Numerical modeling of discontinua, Eng. Comput., 9, 101-113.

[**Error! Reference source not found.**]Cundall, P. A. and Strack, O. D. L. (1979), A discrete numerical model for granular assemblies, *G'eotechnique,* **29**, 47-65.

[**Error! Reference source not found.**] Cleary, P. W. (1991), Extensions of the hybrid method for granular flows, Proceedings 5th International Computational Techniques and Applications Conference, Adelaide, Australia.

[**Error! Reference source not found.**] Cundall, P. A. (1980), UDEC-A generalized distinct element program for modeling jointed rock, Final Tech. Rep. Eur. Res. Office (US Army Contract DAJA37-79-C-0548), NTIS order No. AD-A087 610/2.

[**Error! Reference source not found.**] Walton, O. R. (1980), Particle dynamics modeling of geological materials, Lawrence Livermore National Laboratory, UCRL-52915.

[**Error! Reference source not found.**] Cundall, P. A. and Hart, R. D. (1985), Development of generalized 2D and 3D distinct element programs for modeling jointed rock, Misc. Paper SL-85-1, US Army Corps of Engineers, SL-85-1.

[**Error! Reference source not found.**] Cundall, P. A. (1988), Formulation of a three-dimensional distinct element model - Part I. A scheme to detect and represent contacts in a system composed of many polyhedral blocks, *Int. J. Rock Mech. Min. Sci. Geomech. Abstr.,* **25**, 107-116.

[**Error! Reference source not found.**] Hart, R., Cundall, P. A., and Lemos, J. (1988), Formulation of a three-dimesional distinct element model - Part II. Mechanical calculations for motion and interaction of a system composed of many polyhedral blocks, *Int. J. Rock Mech. Min. Sci. Geomech. Abstr.,* **25**, 117-125.

[**Error! Reference source not found.**] Cundall, P. A. (2001), A discontinuous future for numerical modeling in geomechanics?, *Proc. Inst. Civ. Eng-Geotech. Eng.,* **149**, 41-47.

[**Error! Reference source not found.**] Antonellini, M. A. and Pollard, D. D. (1995), Distinct element modeling of deformation bands in sandstone, *J. Struct. Geol.,* **17**, 1165-1182.

[**Error! Reference source not found.**] Morgan, J. K. (1999a), Numerical simulations of granular shear zones using the distinct element method 1. Shear zones kinematics and the micromechanics of localization, *J. Geophys. Res.,* **104**, 2703-2719.

[**Error! Reference source not found.**] Morgan, J. K. (1999b), Numerical simulations of granular shear zones using the distinct element method 2. Effects of particle size distribution and interparticle friction on mechanical behavior, *J. Geophys. Res.,* **104**, 2721-2732.

[**Error! Reference source not found.**] Heuze, F. E., Walton, O. R., Maddix, D. M., Shaffer, R. J., and Butkovich, T. R. (1993), Analysis of explosions in hard rocks: the power of discrete element modeling, in *Comprehensive Rock Engineering*, Hudson, J. A., Brown, E. T., Fairhurst, C., and Hoek, E., Pergamon Press, New York, NY, pp. 387-413.

[**Error! Reference source not found.**] Sanderson, D. J. and Zhang, X. (1998), Deformation, damage, and fluid flow in fracture networks and around faults, Fall Meeting of the American Geophysical Union.

[**Error! Reference source not found.**] Morris, J. P. (2003), Review of Rock Joint Models, Lawrence Livermore National Laboratory, UCRL-ID-153650, http://www-r.llnl.gov/tid/lof/documents/pdf/244645.pdf.
[**Error! Reference source not found.**] Morris, J. P., Glenn, L. A., and Blair, S. C. (2002), The distinct element method - application to structures in jointed rock, in *Lecture Notes in Computational Science and Engineering: Meshfree Methods*, **26**, Springer-Verlag, Heidelberg, pp. 291-306.
[**Error! Reference source not found.**] Morris, J. P., Rubin, M. B., Block, G. I., Bonner, M.P. (2005), Simulations of Fracture and Fragmentation of Geologic Materials using Combined FEM/DEM Analysis, *Proceedings of Hypervelocity Impact Symposium*, 2005.
[**Error! Reference source not found.**] Morris, J. P., Rubin, M. B., Blair, S. C., Glenn, L. A., and Heuze, F. E. (2004), Simulations of underground structures subjected to dynamic loading using the distinct element method, *Engng Comput.,* **21**, 384-408.
[**Error! Reference source not found.**] Rubin, M. B. (1995), Numerical solution of two- and three-dimensional thermomechanical problems using the theory of a Cosserat point, in *J. of Math. and Phys. (ZAMP)*, **46**, Casey, J. and Crochet, M. J., Brikhauser Verlag, Basel , pp. S308-S334.
[**Error! Reference source not found.**] Rubin, M. B. (2000), *Cosserat Theories: Shells, Rods and Points, Solid Mechanics and its Applications,* Kluwer, The Netherlands.
[**Error! Reference source not found.**] L. B. Lucy, A numerical approach to the testing of the fission hypothesis, *Astron. J.* 83, 1013 (1977).
[**Error! Reference source not found.**] R. A. Gingold and J. J. Monaghan, Smoothed particle hydrodynamics: Theory and application to non-spherical stars, Mon. Not. R. Astron. Soc. 181, 375 (1977).
[**Error! Reference source not found.**] Monaghan, J. J., 1994, Simulating Free Surface Flows with SPH, *Journal of Computational* Physics, **110**, 399-406.
[**Error! Reference source not found.**] Gray, J. P., Monaghan, J. J. and Swift, R. P., SPH elastic dynamics, Comput. Methods Appl. Mech. Engrg. 190 (2001) 6641-6662.
[**Error! Reference source not found.**] J. P. Morris, P. J. Fox, and Y. Zhu, "Modeling low Reynolds number flows using SPH," J. Comput. Phys. 136, 214-226, (1997).
[**Error! Reference source not found.**] J. P. Morris, "Simulating surface tension with Smoothed Particle Hydrodynamics," Int. J. Numer. Meth. Fluid Flow, 33, 333-353 (2000).
[1] Monaghan, J. J., (1992), Smoothed Particle Hydrodynamics, *Annual Reviews in Astronomy and Astrophysics*, **30**, 543-574.
[**Error! Reference source not found.**] Schoenberg, I. J. (1946), Contributions to the problem of approximation of equidistant data by analytic functions, *Q. Appl. Math.*, **4**, 45.
[**Error! Reference source not found.**] Monaghan, J. J., (1997), SPH and Riemann solvers, *Journal of Computational Physics*, **136** (2), 298-307.
[**Error! Reference source not found.**] J. P. Morris and J. J. Monaghan, "A switch to reduce SPH viscosity," J. Comput. Phys. 136, 41-50, (1997).
[**Error! Reference source not found.**] Benz, W. (1989), Smooth Particle Hydrodynamics: A review, p. 269. Nato Workshop, Les Arcs, France.
[**Error! Reference source not found.**] Martin J. C. and Noyce, W. J., *Trans. Phil. Soc.* **244**, 312 (1952).
[**Error! Reference source not found.**] Nguyen, O. and Ortiz, M. (2002), Coarse-graining and renormalization of atomistic binding relations and universal macroscopic cohesive behavior, *J. Mech. Phys. Solids,* **50**, 1727-1741.

Nelson RB, et al., *Numerical analysis of projectile penetration into boulder screens*, U. S. A. C. o. Engineers, 'Editor'. 1983, U.S. Army Engineer Waterways Experiment Station: Vicksburg, Mississippi, United States

2. Kumano A, Goldsmith W. Behavior of diorite under impact by variously-shaped projectiles. *Rock Mechanics* 1982; **15**: 25-40
3. Block G, Rubin M, Morris J, Berryman J. Simulations of dynamic crack propagation in brittle materials using nodal cohesive forces and continuum damage mechanics in the distinct element code LDEC. *International Journal of Fracture* 2007; **144**: 131-147
4. Rubin MB, *Numerical solution of two- and three-dimensional thermomechanical problems using the theory of a Cosserat point*, in *Journal of Mathematics and Physics (ZAMP)*, J. Casey and M. J. Crochet, Editors. 1995, Brikhauser Verlag: Basel, Switzerland. p. 308-334.

5. Rubin MB, *Cosserat Theories: Shells, Rods, and Points, Solid Mechanics and Applications*. Kluwer: The Netherlands, 2000
6. Rubin M. Numerical solution procedures for nonlinear elastic rods using the theory of the Cosserat point. *International Journal of Solids and Structures* 2001; **38**: 4395-4437
7. Ehlers W, Ramm E, Diebels S, D'Addetta GA. From particle ensembles to Cosserat continua: Homogenization of contact forces towards stresses and couple stresses. *International Journal of Solids and Structures* 2003; **40**: 6681-6702
8. Austin CF, Halsey CC, Berry SL, *Full-scale penetration into semiconfined diorite boulders by a semiarmor-piercing (SAP) bomb and a slender penetrator*, P. W. Department, 'Editor'. 1980, Naval Weapons Center
9. Austin CF, Halsey CC, Berry SL, *Full-scale penetration into semiconfined diorite boulders by a semiarmor-piercing (SAP) bomb*, D. f. t. Navy, 'Editor'. 1981, Naval Weapons Center: China Lake, California. 27.

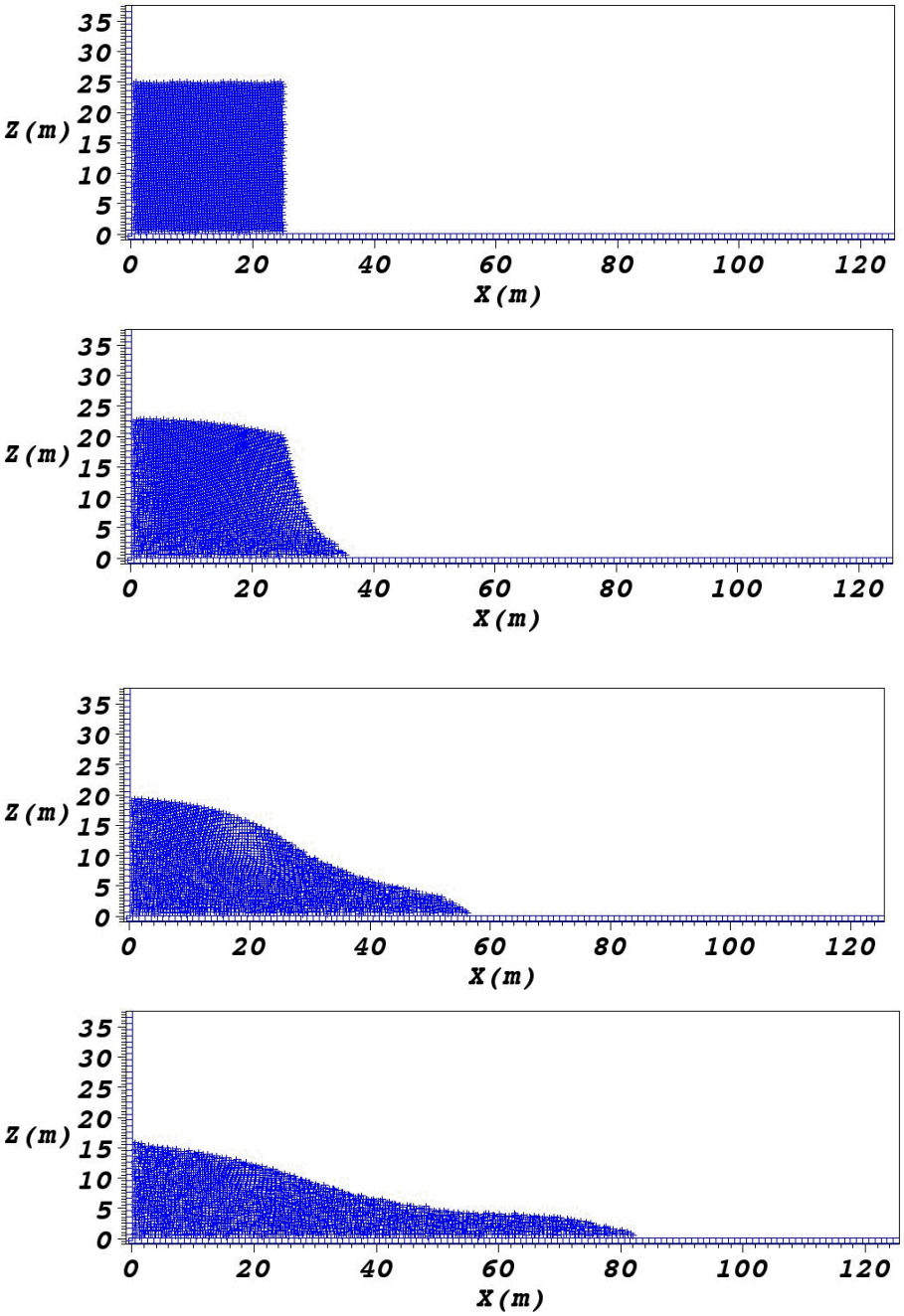

Figure 2: Results of LDEC SPH verification simulation of a 2-dimensional dam burst at 0.0, 0.1, 0.2 and 0.3 seconds.

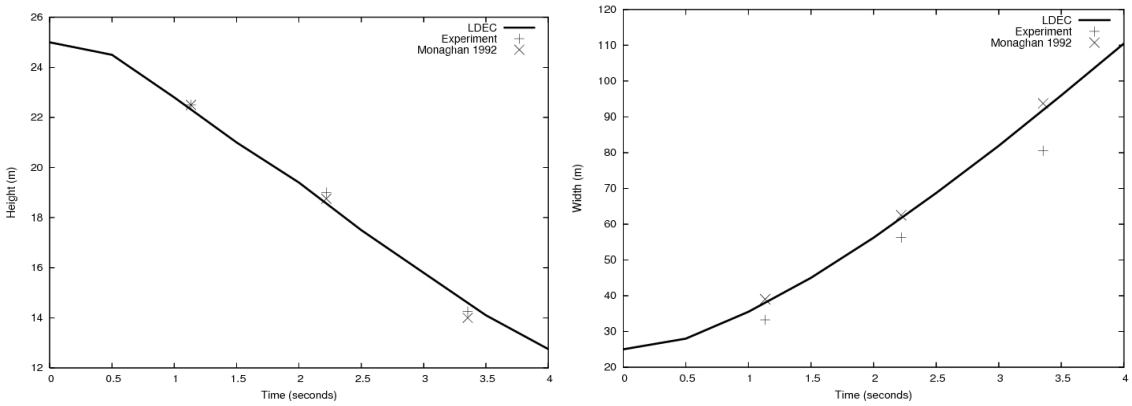

Figure 3: Comparison of a LDEC SPH verification simulation of a 2-dimensional dam burst with experiment and a previous SPH calculation. The LDEC SPH capability is in close agreement with the work of Monaghan [**Error! Reference source not found.**].

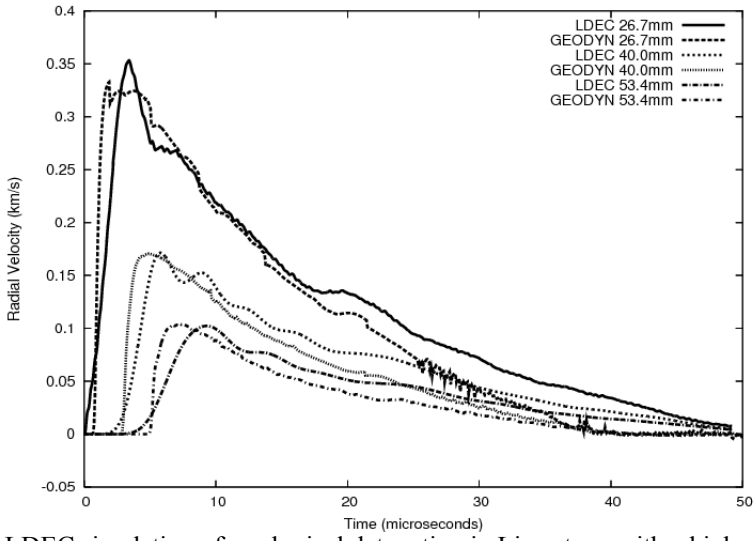

Figure 1 Comparison of a 3-D LDEC simulation of a spherical detonation in Limestone with a high resolution 1-D simulation using GEODYN

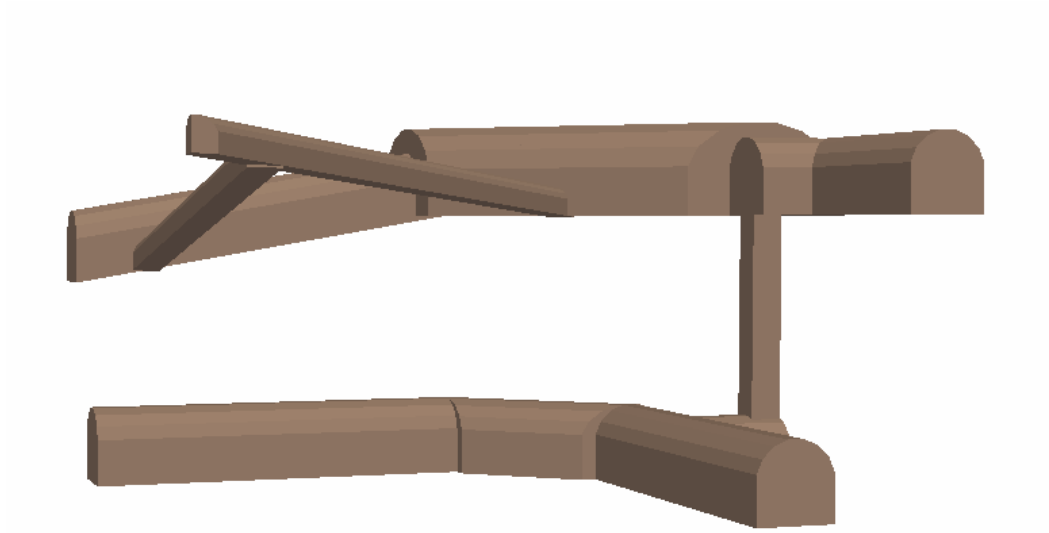

Figure 5: Generic facility model including several tunnel sections and a lift shaft. The facility spans 60m and is buried 50m below the surface.

Figure 6: The non-persistent randomized geology in the vicinity of one of the tunnels. The near-horizontal joint set persists through the model. However, joint sets in the near vertical direction persist only through several consecutive layers at a time.

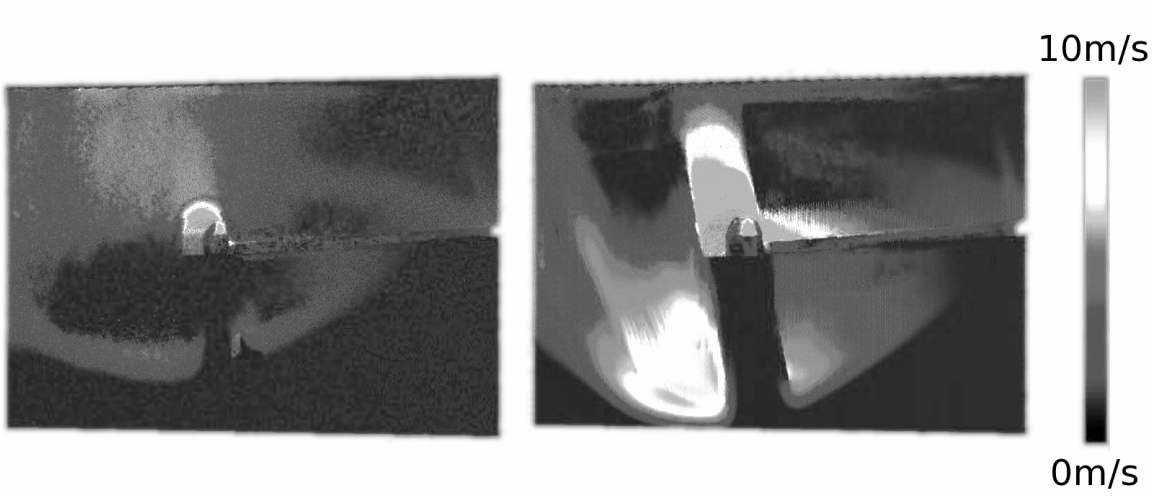

Figure 7: The velocity magnitude for the two models at 30ms. The non-persistent, randomized geology model (left) and the regular jointed model (right) exhibit fundamentally different responses to loading.

Figure 8: Snapshots of the largest room at 0 ms and 200 ms, using the non-persistent joint set simulation. The simulation predicts that this large room within the facility would completely collapse under the applied loading.

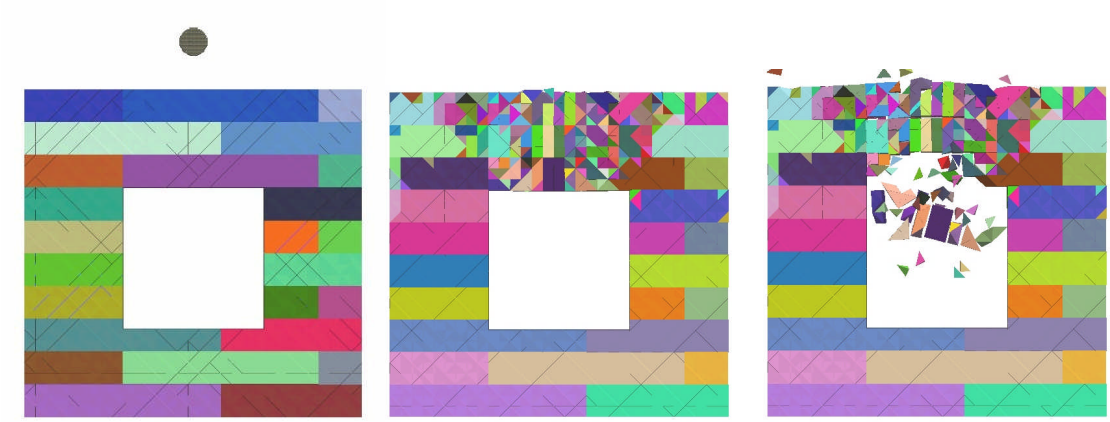

Figure 2: The infrequently jointed model is displayed at far left, with individual blocks colored randomly to emphasize joint locations. The simulation results at 1 ms (middle) show that the initially intact blocks above the tunnel have fragmented. The simulation results at 1 ms (middle) show that the initially intact blocks above the tunnel have fragmented. The simulation at and 100 ms (far right), indicates that a portion of the roof collapses into the tunnel.

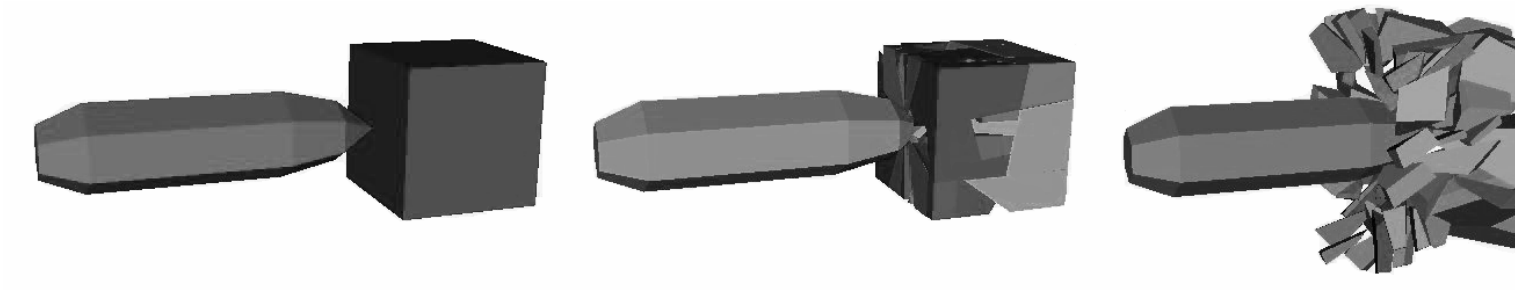

Figure 3: Fragmentation process evolution for impact of projectile into boulder

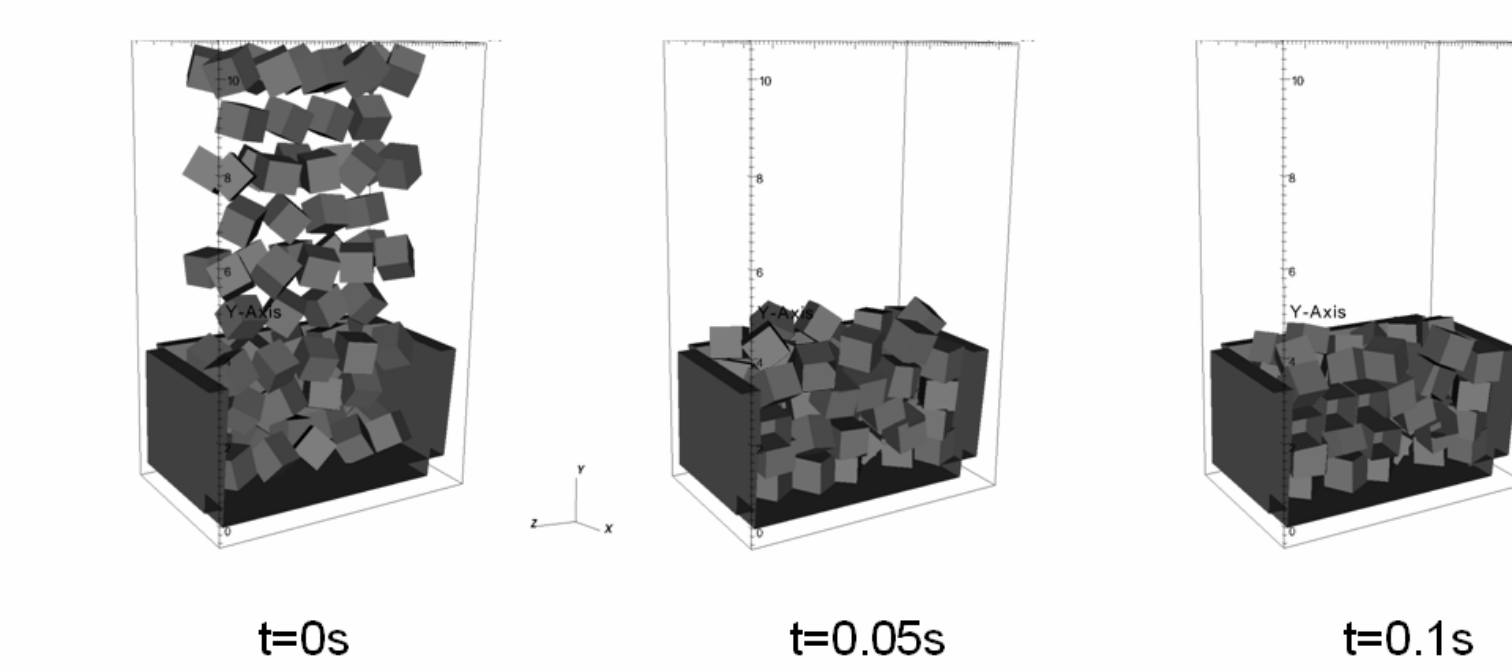

Figure 4: Initialization of the problem domain

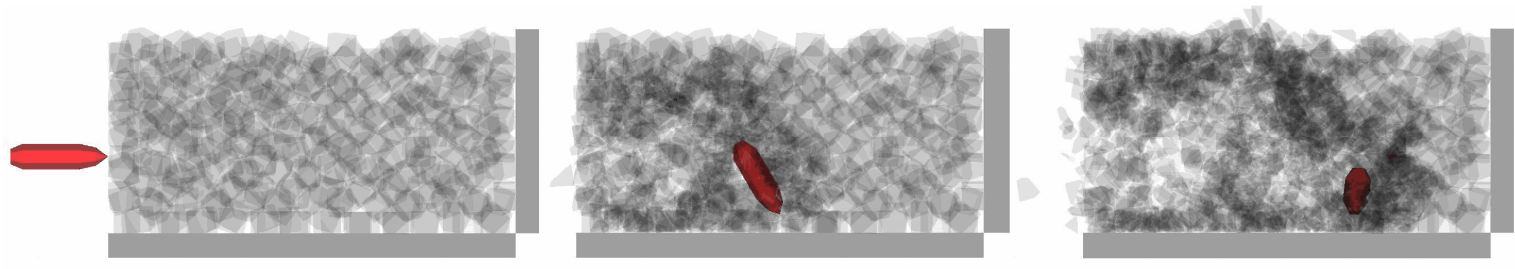

Figure 5: Impact of projectile into a simulated boulder field

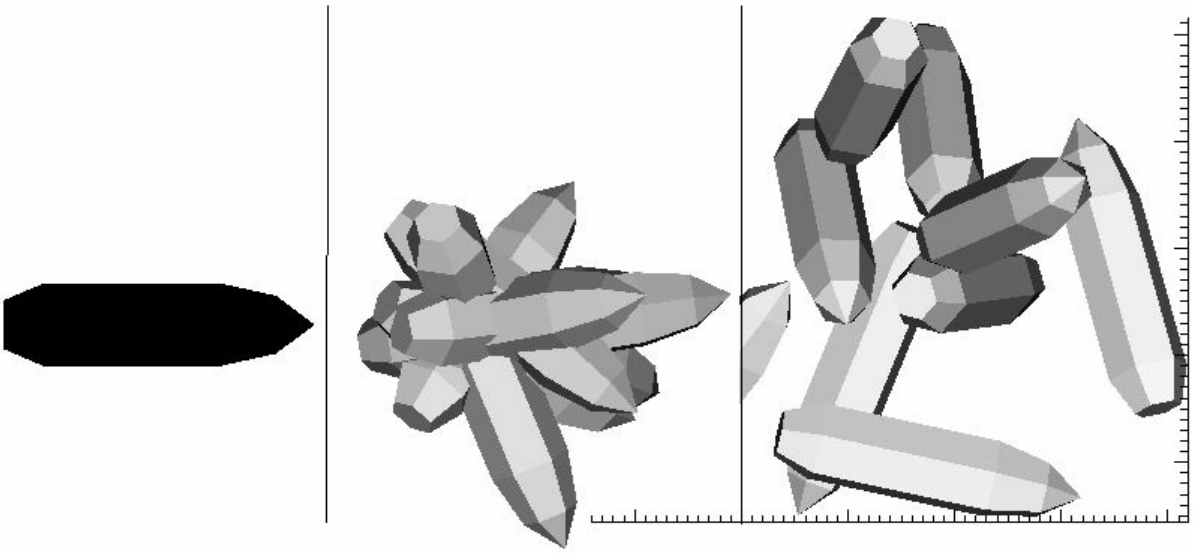

Figure 6: Fate of projectile overlaid for different realizations of the randomly oriented and settled boulder screen for the case of large boulders

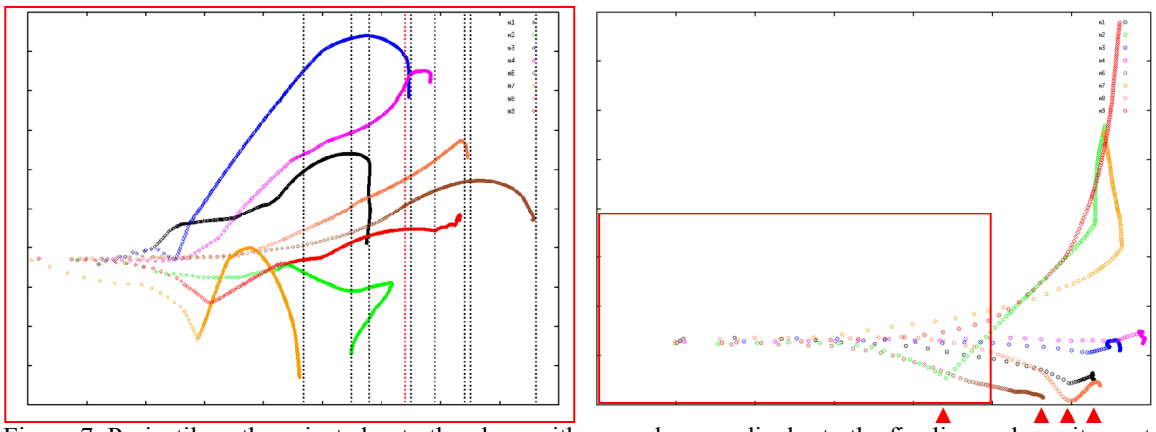

Figure 7: Projectile path projected onto the plane with normal perpendicular to the fire line and gravity vector for different realizations of the randomly oriented and settled boulder screen for the large boulder (left) and small boulder (right) systems.

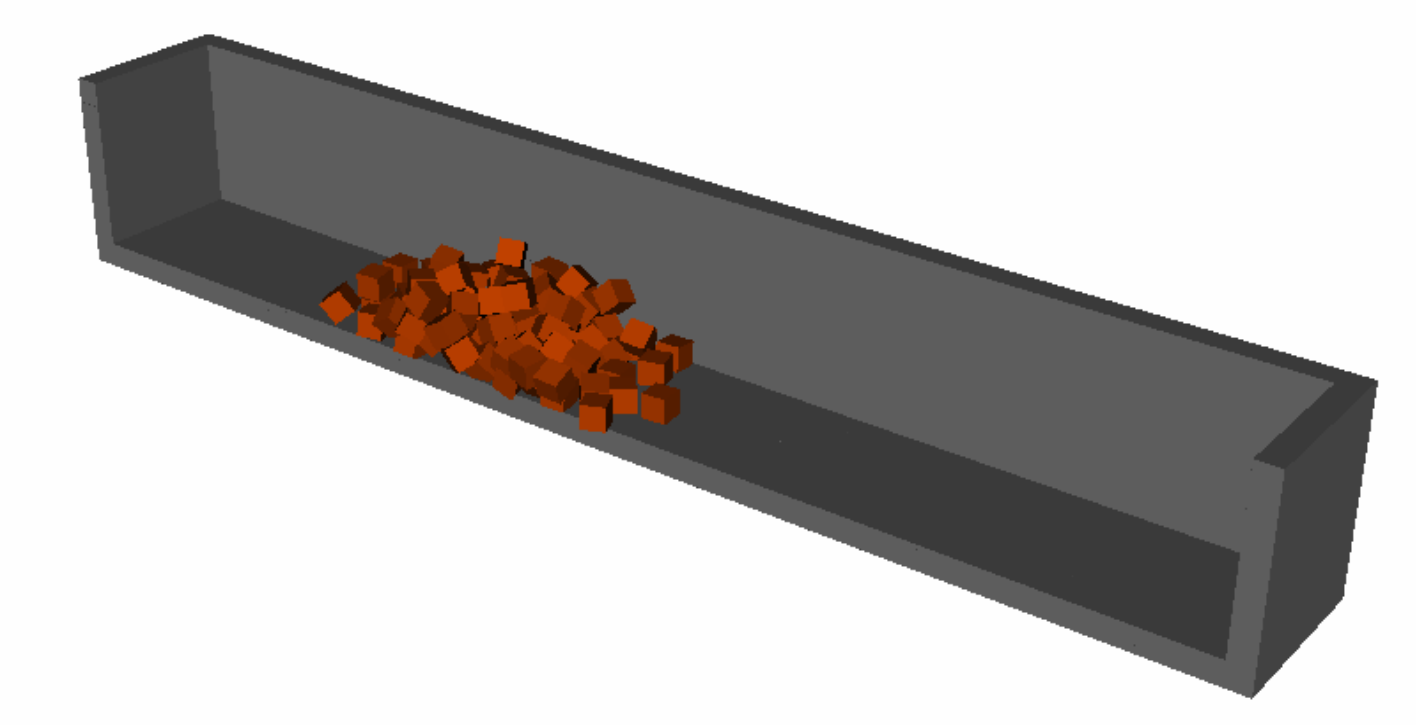

Figure ???: Original arrangement of cubic breakwater units within the computational domain.

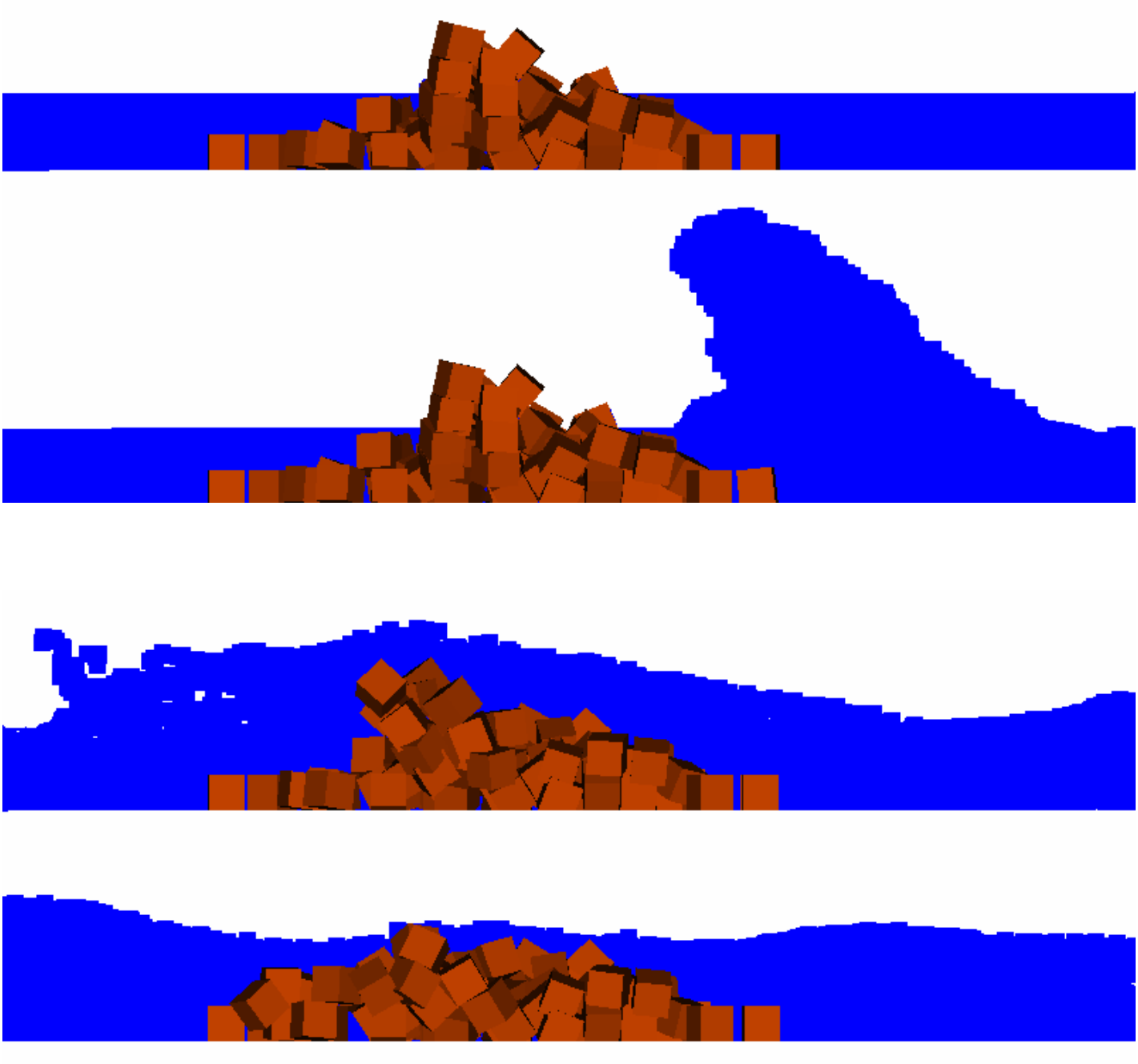

Figure ???: A sequence of snapshots showing the side-view of an LDEC simulation of a wave impinging upon the breakwater configuration depicted in Figure ???. The wave impact upon the breakwater results in boulders being displaced from the top of the structure. Consequently, the height of the breakwater is reduced.

Article section heading (A-head) (Bold, initial cap only, spaces above and below)

Body Text

Quotation

Article subsection heading (B-head) (Bold, initial cap only, spaces above and below)

Article sub-subsection heading (C-head).

Article sub-subsection heading (D-head). (Text continues on same line)

Footnote[1]

1. Footnote text

Authors' Biographies if required for the journal To precede references.

Book reviews **Book title**,
by A.N. Other & John Smith/edited by J. Smith, London, Routledge, 2003,
xliii + 584 pp., US$28.95 (paperback), ISBN X-XXX-XXXXX-X

Reviewer's name
Affiliation
Email

Figure Caption. Figure 1. Initial cap only.

Table Caption

Table 1. Course take-up by sex and socioeconomic classification (%).

	Sex				
Subject	M	F[b]	A	B	C
History	95	5	24.3	60	15.7
Math	27	73	89.8	2[a]	8.2

[a]This is not as accurate, owing to numerical error.
[b]This is an example of a table footnote showing the text turning when the footnote exceeds the table width.

[1] Footnote text.